First Observation of Picosecond Kinetics of Hydrated Electrons in Supercritical Water

ARTICLE *in* JOURNAL OF PHYSICAL CHEMISTRY LETTERS · JANUARY 2010

Impact Factor: 7.46 · DOI: 10.1021/jz900225a · Source: OAI

6 AUTHORS, INCLUDING:

Yusa Muroya
Osaka University
105 PUBLICATIONS **947** CITATIONS
SEE PROFILE

Yosuke Katsumura
The University of Tokyo
268 PUBLICATIONS **2,797** CITATIONS
SEE PROFILE

Mehran Mostafavi
Université Paris-Sud 11
162 PUBLICATIONS **2,902** CITATIONS
SEE PROFILE

THE JOURNAL OF PHYSICAL CHEMISTRY Letters

pubs.acs.org/JPCL

First Observation of Picosecond Kinetics of Hydrated Electrons in Supercritical Water

Yusa Muroya,[†] Mingzhang Lin,[‡] Vincent de Waele,[§,∥] Yoshihiko Hatano,[†] Yosuke Katsumura,*[,†,‡,⊥] and Mehran Mostafavi*[,§,∥]

[†]Nuclear Professional School, School of Engineering, University of Tokyo, 2-22 Shirakata shirane, Tokaimura, Nakagun, Ibaraki 319-1188, Japan, [‡]Advanced Science Research Center, Japan Atomic Energy Agency, 2-4 Shirakata shirane, Tokaimura, Nakagun, Ibaraki 319-1195, Japan, [§]Laboratoire de Chimie Physique/ELYSE, Université Paris-Sud 11, UMR 8000, Bât. 349, Orsay, F-91405, France, [∥]CNRS, Orsay, F-91405, France, and [⊥]Department of Nuclear Engineering and Management, School of Engineering, University of Tokyo, Hongo 7-3-1, Bunkyo-ku, Tokyo 113-8656, Japan

ABSTRACT For the first time, a setup is performed to carry out picosecond time-resolved experiments in supercritical water (SCW) by pulse radiolysis. The kinetics of the decay of the hydrated electron is measured by transient absorption in the near IR on a time-scale ranging from 50 ps to 6 ns. The decay of the hydrated electrons in supercritical conditions shows a fast component at a short time below 500 ps, which is assigned to the reaction of the hydrated electron with the hydronium cation formed by radiolysis. The dependence of the kinetics on the density of SCW is also examined.

SECTION Kinetics, Spectroscopy

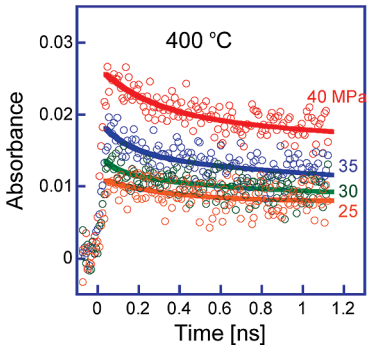

Fluids in supercritical state exhibit physicochemical properties drastically different from those usually observed in the liquid or gas phase. The drastic changes of the thermodynamical parameters of the fluid (density, viscosity, thermal conductance, dielectric constant) also affect the reactivity due to the variation of the diffusion constants, the solvent reorganization, and the possible alteration of the ionic−covalent character of the chemical bonds. For pure water, the supercritical temperature (T_c), pressure (P_c), and density (ρ_v) are T_c = 647.096 K, P_c = 22.064 MPa, and ρ_c = 0.322 g cm^{-3}. Unlike in liquid water, the density of supercritical water (SCW) can be tuned from ρ_v < 0.2 g cm^{-3} (P = 22.5 MPa, T > 650 K), with a gas-like behavior and strong diffuseness through solids, up to ρ_v > 1 g cm^{-3} ($P \geq$ 800 MPa, T = 650 K), with a liquid-like behavior and very strong corrosive properties. SCW is suitable as a substitute for organic solvents in a range of industrial and laboratory processes.[1,2] SCW-cooled reactors[3] are promising advanced nuclear systems to fulfill the requirement of the GenIV nuclear power plant in terms of economics, safety, low waste and proliferation-resistance considerations. An important safety issue in nuclear plant technology is related to the corrosion induced by the coolant, and one aspect of the problem concerns the radiation induced in the fluid in contact with the core nuclear fuel material. Hence, in the course of the development of the nuclear energy, exhaustive experimental and theoretical studies of the radiolysis of H_2O and D_2O under ambient and working conditions of nuclear power plants have been performed.

Under ionizing radiation, water molecules decompose instantaneously into initial radicals (e^-, H_2O^+, $^\bullet$OH and H$^\bullet$) that further react to form the so-called radiolytic species: $H_2O \rightarrow e^-_{aq}$ (hydrated electron), H_3O^+, $^\bullet$OH, H$^\bullet$, H_2, and H_2O_2. These species are initially concentrated into nanometric-size volume, so called "spur," stochastically distributed along the radiation tracks, and then diffused into the bulk solution. In pure water, under ambient conditions, it takes hundreds of nanoseconds to attain the complete homogeneous distribution of species in the fluid. Radiation chemists use the concept of time-dependent G-value (in mol Gy^{-1}) to describe the temporal evolution of concentration of species and the reactivity of a system upon ionizing radiation. In recent years, after the exploration of high-temperature radiolysis below a critical point,[4−8] several studies have aimed to determine the radiolytic yield of each species produced in the water radiolysis by numerous scavengers and pulse radiolysis methods.[9−19] It was found that the radiolytic yield of hydrated electrons and $^\bullet$OH after spur reactions, i.e., at around 100 ns, increases with increasing temperature. Recently, a report compiling all data concerning spur reaction at high temperature below a critical point has been reported.[20] The yields of H_2, H$^\bullet$, and hydrated electrons were also determined in supercritical conditions, using N_2O as a scavenger by measuring systematically gas evolution.[21] However, because of the lack of precise determination of the rate constants for the reactions between radicals and scavengers, the time scale of scavenging corresponding to the G-value at elevated temperature is not very clear throughout different works. The

Received Date: November 5, 2009
Accepted Date: November 25, 2009

DOI: 10.1021/jz900225a | *J. Phys. Chem. Lett.* 2010, *1*, 331–335

scavenging method in SCW is, however, questionable. Indeed, the chemistry of standard scavengers is often unknown under SCW water conditions, and also the presence of a solute at high concentration changes the thermodynamics of the supercritical fluids. In addition to the experimental approaches, computer simulations were performed to predict the water radiolysis decomposition at elevated temperatures; however, large discrepancies between the different simulation methods exist.[22−25]

The time-dependent *G*-values can be determined directly by pulse-radiolysis measurements. However, until now, pulse-radiolysis in SCW was limited to the nanosecond−microsecond time-scale,[26] and thus provided poor information concerning the initial energy deposition process. Recently, the first pulse radiolysis measurements with picosecond electron pulse have been reported in water at high temperatures up to 350 °C and high pressure (25 MPa), opening the route for pulse−probe transient absorption experiments in SCW.[27] While encouraging, this previous study was limited to the SCW regime because of different experimental conditions (low energy (9 MeV) of the accelerated electrons beam, high-temperature flowing cell design, and pump−probe acquisition scheme). By using the 22 MeV LINAC, and the experimental advances, we successfully explored for the first time the chemistry in SCW by using time-resolved measurements with a picosecond time-resolution. The reactivity of the hydrated electron formed by pulse-radiolysis of SCW was probed by transient absorption measurements under different temperature, pressure, and density conditions. This work demonstrates the feasibility of ultrafast pump−probe experiments in SCW as a tool to study many chemical reactions that are accelerated in SCW and in which rate constant cannot be extrapolated from the value known under ambient conditions.

The kinetics of hydrated electrons is followed at the different temperatures and, in SCW, at different densities. Figure 1 shows the temporal behaviors of hydrated electrons in a time range of tens of picoseconds to 5 or 6 ns from room temperature to supercritical conditions. Because the 22 MeV electron beam is not strongly scattered by entering the high-temperature/high-pressure optical flow cell (HTHP-OFC), the dose deposition is higher, and the time-resolution is better than that in ref 27.

At short times, the kinetics is significantly accelerated with increasing temperature. At longer times, the decay is less sensitive to the temperature (solid lines in Figure 2). The parameters of the fits are reported in Table 1. The first time constant decreases with increasing temperature (Table 1). At room temperature during the first 6 ns, the decay of solvated electrons is similar to that already reported by Bartels et al.[28,29] The first fast decay observed at high temperature reported here was not observed in a previous study[27] due to a lower time-resolution of the setup.

One of the most important features of SCW is that its properties depend not only on temperature but also on pressure. We were also able to investigate the pressure dependence of the decay kinetics of a hydrated electron at 400 °C from 40 to 25 MPa (Figure 3). It is noted that the density of D_2O at 400 °C/25 MPa is only 0.182 g/cm^3. The

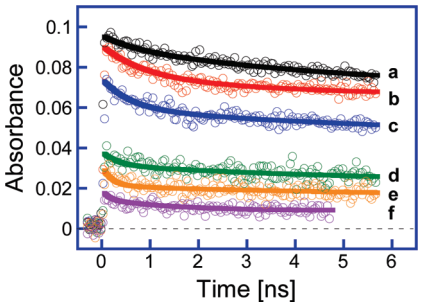

Figure 1. Temporal behaviors of the hydrated electron over 6 ns at different temperatures from room temperature to supercritical conditions measured at different wavelengths under different pressure conditions: (a) 22 °C, 25 MPa, 700 nm; (b) 150 °C, 25 MPa, 860 nm; (c) 250 °C, 25 MPa, 940 nm; (d) 350 °C, 25 MPa, 940 nm; (e) 380 °C, 30 MPa, 940 nm; (f) 400 °C, 30 MPa, 940 nm.

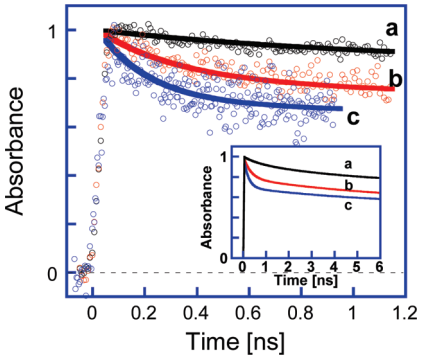

Figure 2. Fast decay kinetics of the hydrated electron within 1.2 ns at different temperatures (normalized signal): (a) 22 °C/25 MPa 700 nm; (b) 300 °C/25 MPa 920 nm; (c) 380 °C/30 MPa 920 nm. Inset: the biexponential fitting curves over 6 ns at each condition: (a) 22 °C/25 MPa at 700 nm; (b) 300 °C/25 MPa at 920 nm; (c) 380 °C/30 MPa at 920 nm.

Table 1. The Fit Parameters for the Decay Reported on the Inset of Figure 2

conditions	fit of kinetics
22 °C/25 MPa	$0.71 \times (1 + 0.080 \times \exp(-t/0.655) + 0.32 \times \exp(-t/5.36))$
300 °C/25 MPa	$0.55 \times (1 + 0.407 \times \exp(-t/0.308) + 0.43 \times \exp(-t/6.41))$
380 °C/30 MPa	$0.517 \times (1 + 0.645 \times \exp(-t/0.20) + 0.35 \times \exp(-t/6.07))$

decay of the hydrated electron measured at 940 nm slows down when the pressure decreases from 40 to 25 MPa. That shows the important density effect on the kinetics of a hydrated electron. The experiments were carried out under the same beam conditions with controlling the irradiation dose, to measure the time profiles of the hydrated electron in the different conditions presented in Figure 3.

According to previous studies by deterministic diffusion−kinetic modeling and stochastic Monte Carlo simulations, the temperature-dependent behavior of a hydrated electron is due to the increase of the competition between the initial size of the spurs, the accelerated diffusion of the

DOI: 10.1021/jz900225a | J. Phys. Chem. Lett. 2010, 1, 331–335

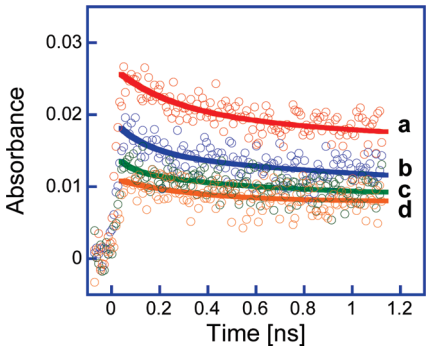

Figure 3. Decay kinetics of a hydrated electron in D_2O at 400 °C under different pressures: (a) 40 MPa, (b) 35 MPa, (c) 30 MPa, and (d) 25 MPa. The measuring wavelength was 920 nm.

species, and the temperature-activated recombination. To rationalize our observation at a first glance in water, we have to consider three main reactions involved in the decay of the hydrated electron:

$$e_{aq}^- + {}^{\bullet}OH \rightarrow OH^- \quad (1)$$

$$e_{aq}^- + H^+ \rightarrow H^{\bullet} \quad (2)$$

$$e_{aq}^- + e_{aq}^- + 2H_2O \rightarrow H_2 + 2OH^- \quad (3)$$

It is reported that the contribution of reaction 1 to the decay of e_{aq}^- becomes less and less important as the temperature increases.[24] This is due to the fact that the rate constant for this reaction increases much less steeply with temperature than the diffusion coefficient of the individual species. The rate constant of reaction 1 at 350 °C is reported to be 4.5×10^{11} L mol^{-1} s^{-1}. As a consequence, more and more hydrated electrons are available as the temperature increases, to either react in other spur reactions (mostly in reactions 2 or 3) or escape into the bulk. The contribution of the self-reaction 3 decreases because, above 200 °C, the rate constant of this reaction drops to less than 10^{10} or 5×10^8 L mol^{-1} s^{-1} according to Christensen and Sehested[6] or Marin et al.,[30] respectively. According to recent experimental measurements[31] below supercritical conditions, the rate constant of reaction 2 increases highly with non-Arrhenius behavior, and reaction 2 becomes the main channel of decay of the hydrated electrons. The rate constant of reaction 2 at 350 °C is 2×10^{12} L mol^{-1} s^{-1}.

From our measurements, it appears that the rate of reaction 2 at 400 °C becomes even faster than that at 350 °C. In SCW, reaction 1, which is the predominant one at room temperature, loses its efficiency in favor of reaction 2. This observation could imply that, for higher temperatures (T > 350 °C), the temperature dependence reported at lower temperatures for k_1 and k_2 can be assumed. In fact, it is known that the dielectric constant of water decreases with increasing temperature. At 350 °C, the dielectric constant of water is 21, but at 400 °C and with a pressure of 25 or 40 MPa, the dielectric constant is reduced to only 2.5 or 9, respectively. The Onsager radius, which depends on the dielectric constant and on the temperature, is increased from 7 to 99 Å, by

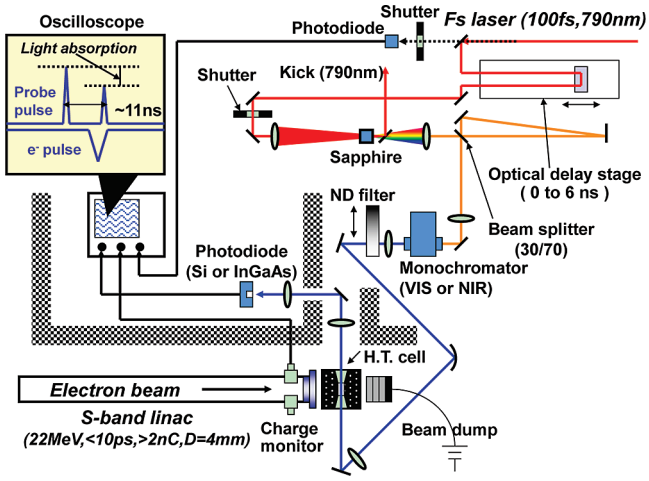

Figure 4. Schematic diagram of the pulse-and-probe picosecond pulse radiolysis system for time-resolved high-temperature/high-pressure measurements.

increasing room temperature up to 400 °C at 25 MPa. In SCW, the electron thermalization distance could be larger than at room temperature (around 20 Å), but because of the lower screening of the columbic interaction with H^+, the escape probability for a solvated electron is strongly reduced. We already reported such a fast decay in the picosecond range for a solvated electron in tetrahydrofuran (THF)[32] at room temperature, which has a low dielectric constant (ε_{THF} = 7.8) close to that of water at 400 °C and 40 MPa. Therefore, the fast decay observed at short times (less than 500 ps) can be mostly due to reaction 2. The pressure-dependent kinetics of the hydrated electron decay in SCW is reported in Figure 3. It is worth noting that as the density of SCW is decreased, the decay of a hydrated electron at short time (< 500 ps) becomes slower. In fact, in SCW, the medium becomes more inhomogeneous, and, mostly when the density is low, SCW has gas-like behavior, then the cage effect loses its efficiency and the "solvated electron" can escape from the spur reaction more easily.[33,34]

The direct observation of reactive species in SCW by picosecond pulse radiolysis, i.e., the effect of temperature and density on the kinetics of hydrated electrons, is very useful in general for mastering the chemistry of the SCW. It is also needed in particular to provide the community with data required for developing realistic models capable of predicting with accuracy the evolution of SCW systems under ionizing radiation, like in future GenIV nuclear power plants. Certainly there is much more quantitative information that can be derived from the various signals. We will soon develop these experimental results to determine the time-dependent yield of hydrated electrons at different temperatures and in SCW. Moreover, the determination of the rate constant of reactions 1 and 2 are under investigation in SCW by picosecond pulse radiolysis.

The experiments were carried out using a newly equipped picosecond pulse radiolysis system, based on a pulse-and-probe method associated with an HTHP-OFC at the Nuclear Professional School of the University of Tokyo (Figure 4). Since H_2O has an absorption around 1100 nm, we used

DOI: 10.1021/jz900225a | J. Phys. Chem. Lett. 2010, 1, 331–335

deuterated water D_2O, because we also measured the absorption spectrum of hydrated electrons at high temperatures. These results are not reported in this letter.

In this pulse−probe scheme, the transient species are generated by an ionizing electron pulse, while the transient absorption is detected by a femtosecond laser pulse. Detailed characteristics and performances of the accelerator and of the synchronization system have been described elsewhere.[35] An HTHP-OFC is placed in front of the exit window of the accelerator, and coupled to the pulse probe setup. The sample chamber is cylindrical (ϕ = 6 mm) with a volume of ~0.6 cm^3 delimited by two 8 mm-thick transparent sapphire windows. The electron beam size is about 3 mm in diameter. After penetrating a 2 mm stainless steel wall, the beam is slightly dispersed. Thus the effective optical path length is about 5−6 mm (calculated by EGS5 codes). In this setup, there is almost no absorption effect of the sapphire windows because the electron beam is well focused, and the electron beam and analyzing light are perpendicular.

The flow system is composed of a high-performance liquid chromatography (HPLC) pump, a preheater, a heater, a power supply with a temperature control unit, and a back-pressure regulator for controlling the temperature and the pressure with a accuracy of 1 °C and 0.1 MPa, respectively, up to 400 °C and 40 MPa.

After the supercontinuum light generation, a beam splitter is used to generate a reference and signal pulses, respectively. The latter is optically delayed by 11 ns from the signal pulse, and both are steered onto the same optical path inside the HTHP-OFC. By adopting this configuration, similar to the "double pulse" setup of Osaka University,[36] the measurements are less sensitive to the rapid instability of the fluid density that are inherent to this type of experiment and that result in the degradation of the optical probe signal. The use of the double pulse is much more decisive under HTHP conditions. Because, unlike ambient conditions, for any solutions that fluctuate dynamically at HTHP conditions, the light passing through the solution is more prone to be diffracted, which makes it difficult to observe accurate light absorption, resulting in degradation of signal-to-noise (S/N) ratio. Since the double pulses pass through the same trajectory with a short time interval (ca. 11 ns), they should be diffracted in a similar manner. That is why, even if the spatial position of the light at the photodiode fluctuates more or less as a result of the diffraction, their measured relative intensity ratio should be insensitive to the fluctuation, which can avoid the degradation of the S/N ratio efficiently, even under HTHP conditions. Four shots are averaged to obtain the signals. Thanks in part to the use of the double-pulse method, the S/N ratio is higher than 10. The high absorption and good signal quality allow us to measure the decay kinetics of a hydrated electron in SCW, even if the signal decreases dramatically with lowering the density of water in supercritical conditions. The overall time resolution (rise of signal of solvated electron, from 10 to 90%) is about 60 ps, coming from (a) the pulse width of the electron beam (~10 ps), (b) the pulse width of the analyzing light (~20 ps), and (c) the difference between the path lengths of the laser and electron beam while passing through the sample (~30 ps).

AUTHOR INFORMATION

Corresponding Author:

*To whom correspondence should be addressed. E-mail: mehran.mostafavi@lcp.u-psud.fr (M.M.); katsu@n.t.u-tokyo.ac.jp (Y.K.).

ACKNOWLEDGMENT We are grateful to T. Ueda, K. Yoshii, and Professor M. Uesaka for their technical assistance in the pulse radiolysis experiments. We also warmly thank Dr. S. Yamashita, Mr. Y. Kumagai, and Mr. K. Hata for their help in experiments.

REFERENCES

(1) Eckert, C. A.; Knutson, B. L.; Debenedetti, P. G. Supercritical Fluids as Solvents for Chemical and Materials Processing. *Nature* **1996,** *383*, 313–318.

(2) Akiya, N.; Savage, P. E. Roles of Water for Chemical Reactions in High-Temperature Water. *Chem. Rev.* **2002,** *102*, 2725–2750.

(3) Oka, Y.; Kataoka, K. Conceptual Design of a Fast Breeder Reactor Cooled by Supercritical Steam. *Ann. Nucl. Energy* **1992,** *19*, 243–247.

(4) Gottschall, W. C.; Hart, E. J. The Effect of Temperature on the Absorption Spectrum of the Hydrated Electron and on Its Bimolecular Recombination Reaction. *J. Phys. Chem.* **1967,** *71*, 5.

(5) Michael, B. D.; Hart, E. J.; Schmidt, K. H. The Absorption Spectrum of e^-_{aq} in the Temperature Range −4 to 390 °C. *J. Phys. Chem.* **1971,** *75*, 2798–2805.

(6) Christensen, H. C.; Sehested, K. The Hydrated Electron and Its Reactions at High Temperatures. *J. Phys. Chem.* **1986,** *90*, 186–190.

(7) Elliot, A. J. Rate Constants and G-Values for the Simulation of the Radiolysis of Light Water over the Range 0−300 °C. AECL Report AECL-11073, COG-94-167; 1994.

(8) Buxton, G. V. High Temperature Water Radiolysis. In *Radiation Chemistry: Present Status and Future Trends*; Jonah, C. D.; Rao, B. S. M., Eds.; Elsevier: Tokyo, 2001; pp 145−162.

(9) Burns, W. G.; Marsh, W. R. Radiation-Chemistry of High-Temperature (300−410 °C) Water 1. Reducing Products from Gamma-Radiolysis. *J. Chem. Soc., Faraday Trans. I* **1981,** *77*, 197–215.

(10) Ferry, J. L.; Fox, M. A. Effect of Temperature on the Reaction of $^{\bullet}OH$ with Benzene and Pentahalogenated Phenolate Anions in Subcritical and Supercritical Water. *J. Phys. Chem. A* **1998,** *102*, 3705–3710.

(11) Wu, G.; Katsumura, Y.; Muroya, Y.; Li, X.; Terada, Y. Hydrated Electron in Subcritical and Supercritical Water: A Pulse Radiolysis Study. *Chem. Phys. Lett.* **2000,** *325*, 531–536.

(12) Wu, G. Z.; Katsumura, Y.; Muroya, Y.; Lin, M. Z.; Morioka, T. Temperature Dependence of $(SCN)_2^{\bullet-}$ in Water at 25−400 °C: Absorption Spectrum, Equilibrium Constant, and Decay. *J. Phys. Chem. A* **2001,** *105*, 4933–4939.

(13) Cline, J.; Takahashi, K.; Marin, T. W.; Jonah, C. D.; Bartels, D. M. Pulse Radiolysis of Supercritical Water. 1. Reactions between Hydrophobic and Anionic Species. *J. Phys. Chem. A* **2002,** *106*, 12260–12269.

(14) Marin, T. W.; Cline, J. A.; Takahashi, K.; Bartels, D. M.; Jonah, C. D. Pulse Radiolysis of Supercritical Water. 2. Reaction of Nitrobenzene with Hydrated Electrons and Hydroxyl Radicals. *J. Phys. Chem. A* **2002,** *106*, 12270–12279.

DOI: 10.1021/jz900225a | *J. Phys. Chem. Lett.* **2010,** *1*, 331–335

(15) Bartels, D. M.; Takahashi, K.; Cline, J. A.; Marin, T. W.; Jonah, C. D. Pulse Radiolysis of Supercritical Water. 3. Spectrum and Thermodynamics of the Hydrated Electron. *J. Phys. Chem. A* **2005,** *109*, 1299–1307.

(16) Marin, T. W.; Jonah, C. D.; Bartels, D. M. Reaction of $^{\bullet}$OH Radicals with H-2 in Sub-critical Water. *Chem. Phys. Lett.* **2003,** *371*, 144–149.

(17) Feng, J.; Aki, S. N. V. K.; Chateauneuf, J. E.; Brennecke, J. F. Hydroxyl Radical Reactivity with Nitrobenzene in Subcritical and Supercritical Water. *J. Am. Chem. Soc.* **2002,** *124*, 6304–6311.

(18) Lin, M. Z.; Katsumura, Y.; Muroya, Y.; He, H.; Wu, G. Z.; Han, Z. H.; Miyazaki, T.; Kudo, H. Pulse Radiolysis Study on the Estimation of Radiolytic Yields of Water Decomposition Products in High-Temperature and Supercritical Water: Use of Methyl Viologen as a Scavenger. *J. Phys. Chem. A* **2004,** *108*, 8287–8295.

(19) Lin, M. Z.; Katsumura, Y.; He, H.; Muroya, Y.; Han, Z. H.; Miyazaki, T.; Kudo, H. Pulse Radiolysis of 4,4′-Bipyridyl Aqueous Solutions at Elevated Temperatures: Spectral Changes and Reaction Kinetics up to 400 °C. *J. Phys. Chem. A* **2005,** *109*, 2847–2854.

(20) Elliot, A. J.; Bartels, D. M. The Reaction Set, Rate Constants and g-Values for the Simulation of the Radiolysis of Light Water over the Range 20° to 350 °C. Based on Information Available in 2008, AECL Report No. 153-127160-450-001, 2009.

(21) Janik, D.; Janik, I.; Bartels, D. M. Neutron and Beta/Gamma Radiolysis of Water up to Supercritical Conditions. 1. Beta/Gamma Yields for H_2, $H^{\bullet}$ Atom, and Hydrated Electron. *J. Phys. Chem. A* **2007,** *111*, 7777–7786.

(22) Laverne, J. A.; Pimblott, S. M. Diffusion-Kinetic Modeling of the Electron Radiolysis of Water at Elevated-Temperatures. *J. Phys. Chem.* **1993,** *97*, 3291–3297.

(23) Swiatla-Wojcik, D.; Buxton, G. V. Modeling of Radiation Spur Processes in Water at Temperatures up to 300 °C. *J. Phys. Chem.* **1995,** *99*, 11464–11471.

(24) du Penhoat, M. A. H.; Goulet, T.; Frongillo, Y.; Fraser, M. J.; Bernat, P.; Jay-Gerin, J. P. Radiolysis of Liquid Water at Temperatures up to 300 °C: A Monte Carlo Simulation Study. *J. Phys. Chem. A* **2000,** *104*, 11757–11770.

(25) Meesungnoen, J.; Jay-Gerin, J. P.; Filali-Mouhim, A.; Mankhetkorn, S. On the Temperature Dependence of the Primary Yield and the Product $G\varepsilon_{max}$ of Hydrated Electrons in the Low-LET Radiolysis of Liquid Water. *Can. J. Chem.* **2002,** *80*, 767–773.

(26) Katsumura, Y. Application of Radiation Chemistry to Nuclear Technology. In *Charged Particle and Photon Interactions with Matter*; Mozumder, A.; Hatano, Y., Eds.; Marcel Dekker, Inc.: New York, 2004; pp 697−727.

(27) Baldacchino, G.; De Waele, V.; Monard, H.; Sorgues, S.; Gobert, F.; Larbre, J. P.; Vigneron, G.; Marignier, J. L.; Pommeret, S.; Mostafavi, M. Hydrated Electron Decay Measurements with Picosecond Pulse Radiolysis at Elevated Temperatures up to 350 °C. *Chem. Phys. Lett.* **2006,** *424*, 77–81.

(28) Bartels, D. M.; Cook, A R.; Mudaliar, M.; Jonah, C. D. Spur Decay of the Solvated Electron in Picosecond Radiolysis Measured with Time-Correlated Absorption Spectroscopy. *J. Phys. Chem. A* **2000,** *104*, 1686–1691.

(29) Bartels, D. M.; Gosztola, D.; Jonah, C. D. Spur Decay Kinetics of the Solvated Electron in Heavy Water Radiolysis. *J. Phys. Chem. A* **2001,** *105*, 8069–8072.

(30) Marin, T. W.; Takahashi, K.; Jonah, C. D.; Chemerisov, S. D.; Bartels, D. M. Recombination of the Hydrated Electron at High Temperature and Pressure in Hydrogenated Alkaline Water. *J. Phys. Chem. A* **2007,** *111*, 11540–11551.

(31) Stanisky, C. M.; Bartels, D. M.; Takahashi, K. Rate Constants for the Reaction of Hydronium Ions with Hydrated Electrons up to 350 °C. *Radiat. Phys. Chem.* **2010,** *79*, 64–65.

(32) De Waele, V.; Sorgues, S.; Pernot, P.; Marignier, J. L.; Monard, H.; Larbre, J. P.; Mostafavi, M. Geminate Recombination Measurements of Solvated Electron in THF Using Laser-Synchronized Picosecond Electron Pulse. *Chem. Phys. Lett.* **2006,** *423*, 30–34.

(33) Ghandi, K.; Addison-Jones, B.; Brodovitch, J. C.; McKenzie, I.; Percival, P. W.; Schüth, J. Near-Diffusion-Controlled Reactions of Muonium in Sub- and Supercritical Water. *Phys. Chem. Chem. Phys.* **2002,** *4*, 586–595.

(34) Ghandi, K.; Percival, P. W. Prediction of Rate Constants for Reactions of the Hydroxyl Radical in Water at High Temperatures and Pressures. *J. Phys. Chem. A* **2003,** *107*, 3005–3008.

(35) Muroya, Y.; Lin, M. Z.; Iijima, H.; Ueda, T.; Katsumura, Y. Current Status of the Ultra-fast Pulse Radiolysis System at NERL, the University of Tokyo. *Res. Chem. Intermed.* **2005,** *31*, 261–272.

(36) Saeki, A.; Kozawa, T.; Kashiwagi, S.; Okamoto, K.; Isoyama, G.; Yoshida, Y.; Tagawa, S. Synchronization of Femtosecond UV-IR Laser with Electron Beam for Pulse Radiolysis Studies. *Nucl. Instrum. Methods Phys. Res. Sect. A: Accel. Spectrom. Detect. Assoc. Equip.* **2005,** *546*, 627–633.

DOI: 10.1021/jz900225a | *J. Phys. Chem. Lett.* **2010,** *1*, 331–335